Stabilized helical spin order and multiferroic phase coexistence in $MnWO_4$: Consequence of 4*d* Ru substitution of Mn

H. W. Yu,[1] M. F. Liu,[1] X. Li,[1] L. Li,[1] L. Lin,[1] Z. B. Yan,[1] and J.-M. Liu[1,2,*]

[1]*Laboratory of Solid State Microstructures, Nanjing University, Nanjing 210093, China*

[2]*Institute for Advanced Materials, South China Normal University, Guangzhou 510006, China*

(Received 9 December 2012; revised manuscript received 19 February 2013; published 11 March 2013)

Most earlier work on the effect of chemical substitution in multiferroic $MnWO_4$ has focused on the 3*d* transition metal substitution of Mn. In this paper, we investigate the Ru substitution of Mn in polycrystalline $Mn_{1-x}Ru_{x/2}WO_4$ in order to unveil the consequence of 4*d* transition metal substitution in terms of magnetic transitions and ferroelectricity. It is found that the Ru substitution substantially reshuffles the magnetic frustration and stabilizes the incommensurate helical spin-order phase (AF2) by partially suppressing the collinear spin-order phase (AF1 phase). The coexistence of the AF2 and AF1 phases at low temperature is suggested. Consequently, the ferroelectric polarization is remarkably enhanced, accompanied with significant response of the polarization to magnetic field. It is argued that the structural distortion and enhanced spin-orbital coupling associated with the Ru substitution may be responsible for this ferroelectricity enhancement.

DOI: 10.1103/PhysRevB.87.104404 PACS number(s): 75.30.Kz, 75.85.+t, 77.80.−e

I. INTRODUCTION

The discovery of ferroelectricity in some magnetic transition metal oxides has inspired intensive interest in so-called type-II multiferroics or improper ferroelectrics in which the mutual control of magnetism and ferroelectricity becomes possible, not only due to promising application potentials, but also for understanding the complicated interactions dominating among various ferroic orders.[1–3] A series of novel multiferroics have consequently been discovered, including orthorhombic rare-earth manganites ($RMnO_3$ and RMn_2O_5, R = rare earth),[4–6] triangular cuprates ($LiCuO_2$, $FeCuO_2$, $CrCuO_2$, etc.),[7–9] $Ni_3V_2O_8$,[10] Ca_3CoMnO_6,[11] and so on. The ferroelectricity in these multiferroic oxides is believed to appear mainly due to two microscopic mechanisms. One is the spatial inverse symmetry breaking induced by the spin-orbit coupling (SOC) via the inverse Dzyaloshinskii–Moriya (DM) interaction or equivalently the super spin current scenario,[12,13] mainly identified in 3*d* magnetic transition metal oxides of noncollinear spin order.[14,15] The other is the spin-lattice coupling associated with collinear, typically the ↑↑↓↓ spin order, or E-type antiferromagnetic (AFM) order, which breaks the inverse symmetry, too.[16–18] In particular, those multiferroics of noncollinear spin order have been intensively addressed in the past several years partially because the ferroelectricity is associated with the SOC via the DM interaction, allowing very strong magnetoelectric (ME) coupling.[6]

A common characteristic of these multiferroics is the highly frustrated spin structure, either due to the triangle-like lattice geometry or arising from multifold competing interactions.[19,20] Usually, the competition between the nearest neighbor (NN) interaction and next nearest neighbor (NNN) interaction plus the spin-orbit/spin-lattice coupling results in the serious spin frustration, which allows various spin configurations of similar scales in the energy landscape so that a series of magnetic transitions upon small variation in intrinsic or external degree of freedom, e.g. temperature, pressure, and chemical substitutions, occur in sequence.[21,22] For example, the noncollinear spiral spin order in orthorhombic manganites (Tb, Dy)MnO_3 is determined mainly by the competing NN Mn-O-Mn and NNN Mn-O-O-Mn interactions,[19,23] and a similar case applies to other multiferroics of noncollinear spiral/helical spin orders. While these spin-frustrated multiferroics offer an advantage that the spin structure and thus the ferroelectricity are sensitive to the external magnetic field, which benefits the magnetic field control of ferroelectric polarization, the due disadvantage is the low stability of spin structure and then the low ferroelectric (FE) Curie temperature (T_{FE}).

One of the representative and well-studied multiferroic materials embracing those characteristics addressed above, besides the abovementioned manganites, is $MnWO_4$ (monoclinic, $P2/c$).[24] It accommodates the distorted stacking of $Mn^{2+}O_6$ octahedral with W^{6+} ions filled in-between. It was surprisingly found that the Mn^{2+}-Mn^{2+} spin interaction can even sustain over the 11th neighbors,[25] making the interaction competition very complicated and thus leading to highly frustrated spin structures which are likely sensitive to perturbations. It was observed that $MnWO_4$ first enters a very narrow collinear but incommensurate (ICM) antiferromagnetic (AFM) structure (AF3 phase) with wave vector $q_3 = (0.214, 0.5, -0.457)$ and sinusoidally modulated spin moment at temperature $T = T_{AF3} \sim 13.5$ K from the high-T paramagnetic phase, and then an ICM noncollinear spin structure (AF2 phase) with wave vector $q_2 = q_3$ is favored at $T < T_{AF2} \sim 12.6$ K,[24,26] leaving only a 1-K gap between the two consecutive magnetic transitions. This AF2 phase accommodates an FE polarization (P) aligning along the b axis, owing to the abovementioned SOC mechanism via the DM interaction. The maximal P is only $\sim 50\ \mu C/m^2$.[27] At $T < T_{AF1} = 7$ K, this FE AF2 phase is again replaced by a commensurate (CM) AFM phase (AF1) which is unfortunately free of FE polarization. The corresponding lattice structure and spin configurations in the three phases are schematically given in Figs. 1(a)–1(d), where the lattice distortion may be exaggerated for a guide to the eyes.

Therefore, $MnWO_4$ plays as an attractive platform for us to modulate the frustrated interactions and consequent

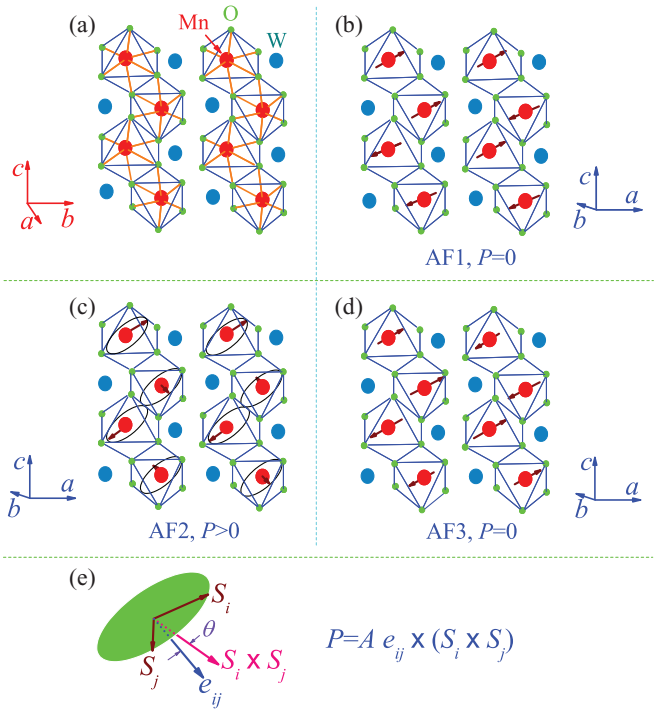

FIG. 1. (Color online) Schematic drawing of the lattice and spin structures of $MnWO_4$: (a) crystal structure, each Mn is surrounded by an oxygen octahedron, and the W ions separate the zigzag Mn chains along the c axis; (b) spin structure of the AF1 phase with the moments on the ac plane with an angle of $\sim 35^\circ$ from the a axis; (c) spin structure of the AF2 phase with a helical order; and (d) spin structure of the AF3 phase with the moment direction identical to that in the AF1 phase but the moment amplitude modulated. The as-generated polarization P along the b axis and the helical spin rotation plane are shown in (e), with the chirality vector $(S_i \times S_j)$ and the Mn-Mn separation vector e_{ij}.

multiferroic behaviors via various approaches. We address here the effect of chemical substitution as an approach to such modulations. Experimental results have demonstrated the tremendous impact of an even slight Mn^{2+} substitution by $3d$ transition metal ions (Fe, Co, Ni, Cu, Zn, etc.).[28–31] It seems to us that the magnetic ion substitution most likely induces even more complicated magnetic interactions and thus leads to more magnetic phase transitions. The extremely low level nonmagnetic substitution tends to stabilize the FE AF2 phase by suppressing the non-FE AF1 phase, while this advantage is limited since a relatively high substitution would eventually break the spin order.

It should be mentioned that the FE AF2 phase is highly favored from a consideration of multiferroicity, and thus the highly frustrated spin structure should be modulated in order to stabilize this phase. One example is the Co substitution, which does stabilize the AF2 phase by suppressing the AF1 phase at a proper substitution level. However, this case also leads to appearance of additional magnetic phases such as AF4 and AF5 in the high substitution level, although the AF5 phase was found to be ferroelectric.[32,37] Therefore, searching for alternative substitution, which can stabilize the AF2 phase by reshuffling the spin interactions in order to enhance the ferroelectricity, is appealed.

Along this line, one notes that reported experiments on the chemical substitution mainly focus on $3d$ magnetic transition metal ions which offer strong magnetic interactions and big on-site Coulomb energy. These may allow us to modulate the stability of the FE AF2 phase on one hand; on the other hand, the SOC effect can be enhanced since the strong SOC is required for ferroelectricity.[32] One potential alternative is the substitution by $4d$ transition metal ions like Ru^{4+}. The motivation is threefold. First, $4d$ and even $5d$ magnetic ions in oxides usually exhibit magnetic moments different from the strongly correlated $3d$ ions, benefiting modulation of the spin frustration. Second, the relatively strong SOC of $4d$ ions allows a possibility of enhancing FE polarization via the inverse DM interaction since the DM coefficients of those $4d$ oxides are generally big.[33] Third, it has been repeatedly identified that the p-d orbit hybridization can be an essential ingredient for generating electronic dipole polarization, which seems to be the origin for ferroelectricity in multiferroic $CuFeO_2$, etc.[34] The $4d$ ions usually have more extended charge distribution than the $3d$ ions, thus allowing stronger p-d hybridization. Surely, for $5d$ ions, the charge distribution may be overextended, unfavoring the insulating state required for ferroelectricity, while these multiferroics usually have a band gap less than 1.0 eV.[35] In summarizing these considerations, an investigation on the effect of Ru^{4+} substitution of Mn^{2+} in $MnWO_4$ is needed.

It should be also noted that the Mn spin rotation plane is nearly perpendicular to the separation vector e_{ij} between two Mn neighboring spins. In Fig. 1(e), we plot the spin rotation plane where the spin chirality $(S_i \times S_j)$ and e_{ij} are labeled, with an angle θ between the screw axis and e_{ij}. The generated polarization along the b axis is $P = A \cdot e_{ij} \times (S_i \times S_j)$, where A is the SOC constant. It is seen that the magnitude of P is substantially dependent on angle θ in geometry, but this angle may be small for $MnWO_4$ due to the zigzag Mn-Mn chain along the c axis. It is therefore expected that increasing SOC constant A by enhancing the SOC on one hand and modulating the lattice distortion on the other hand so that angle θ can be enlarged are both beneficial to the enhancement of the P magnitude.

In this paper, we perform extensive experiments on the structural, magnetic, and ferroelectric consequences of $Mn_{1-x}Ru_{x/2}WO_4$ by keeping the charge neutrality upon the Ru^{4+} substitution in the macroscopic sense. It will be shown that the Ru^{4+} substitution of Mn^{2+} does stabilize the AF2 phase by partially suppressing the AF1 phase and the AF1 + AF2 phase coexistence at low T, while the high-T AF3 phase remains roughly unaffected. More importantly, we observe remarkable enhancement of the FE polarization due to the substitution. The value of P at $T = 2$ K for polycrystalline $Mn_{1-x}Ru_{x/2}WO_4$ at $x = 0.20$ reaches up to 60 $\mu C/m^2$, almost one order of magnitude higher than pure or Co-substituted $MnWO_4$ in polycrystalline form. Although the details of the magnetic structure evolution upon the substitution remain open at this stage, our motivations on the Ru^{4+} substitution seems to be generally supported.

The remaining part of this paper is organized as follows. In Sec. II, we describe relevant sample preparation and characterizations. The main results are presented in Sec. III. We present an explanation on the possible mechanism in Sec. IV

together with a comprehensive magnetic phase diagram. A brief conclusion is given in Sec. V.

II. EXPERIMENTAL DETAILS

In $MnWO_4$, Mn^{2+} ion is ~0.080 nm in radius, and that for W^{6+} is 0.062 nm. The ionic radius of Ru^{4+} is 0.067 nm, slightly smaller than that of Mn^{2+}. Therefore, the Ru substitution of Mn will result in more serious lattice distortion in addition to the lattice contraction. In this case, a high-level substitution becomes difficult also. We successfully synthesized $Mn_{1-x}Ru_{x/2}WO_4$ polycrystalline samples with x as high as 0.20, over which clear impurity phase is detected. It is addressed once more that chemically one Ru^{4+} substitutes two Mn^{2+} ions for the charge neutrality consideration in the macroscopic sense, while such a substitution may result in local Mn^{2+} deficiency or oxygen vacancies since one Ru^{4+} ion is supposed to replace two Mn^{2+} ions.

The samples were prepared by conventional solid state sintering. Substantial efforts were made to optimize the synthesis parameters since species Ru is easy to evaporate during the sintering. In sequence, stoichiometric amounts of high-purity WO_3, RuO_2, and MnO were chosen as reagents and were thoroughly mixed for 24 h. Then the mixture was grounded for 1.0 h and then annealed in air for 12 h at 600 °C. After an additional several times of intermediate grinding and sintering at 600 °C for 12 h, the output mixture was compressed to pellets with a diameter of 20 mm, and annealed at 950 °C for 20 h in air. The spontaneous cooling down to room temperature yielded the as-prepared samples.

The as-prepared sample series were checked using x-ray diffraction (XRD; Bruker Corporation) equipped with Cu K_α radiation. By comparing the detected θ-2θ spectrum with the standard database, one is able to evaluate the lattice constants as functions of substitution level x. In addition, we performed x-ray photoelectron spectroscopy (XPS) measurements on the chemical composition and species valences of the samples, and only those stoichiometric samples were chosen for subsequent characterizations.

Extensive measurements on the specific heat, magnetization and magnetic susceptibility, dielectric, and ferroelectric properties were carried out. The magnetization M and magnetic susceptibility χ were measured using the Quantum Design Superconducting Quantum Interference Device (SQUID) in the zero-field-cooled (ZFC) mode and field-cooling (FC) mode, respectively. The cooling field and measuring field are both 1000 Oe. The specific heat C_p was measured using the Physical Properties Measurement System (PPMS) in the standard procedure.

Because $MnWO_4$ exhibits ferroelectricity only at low T, the pyroelectric current (I) method was used to probe the polarization P. Each sample was polished into a thin disk of 0.2 mm in thickness and then sandwich-coated with Au layers as top and bottom electrodes. The measurement was performed using the Keithley 6514A electrometer connected to the PPMS. In detail, each sample was submitted to the PPMS and cooled down to ~100 K. Then a poling electric field of ~10 kV/cm was applied to the sample until the sample was down to ~2 K, at which the sample was short-circuited for ~60 min in order to release any charges accumulated on the sample surfaces or inside the sample. Then the sample was heated slowly at a warming rate, during which the pyroelectric current I was collected. Identical measurements were performed with different warming rates from 1 to 6 K/min, and the collected data are compared to ensure no contribution other than the pyroelectric current. The validity of this procedure was confirmed and repeated in earlier works[36] and will be shown below, too. At the same time, the dielectric susceptibility ε at various frequencies as a function of T was collected using the HP4294A impedance analyzer.

Besides the P-T data, we also measured the response of P to magnetic field H in two modes. One is the isothermal mode with which the variation in P in response to the scanning of H was detected, and the other is the iso-field mode with which the P-T data under a fixed H were collected. By such measurements, one can evaluate the magnetoelectric (ME) coupling of the materials.

III. RESULTS AND DISCUSSION

A. Structural distortion

First, we present the measured XRD θ-2θ spectra at room temperature for the $Mn_{1-x}Ru_{x/2}WO_4$ sample series in Fig. 2(a), where the local (002) and (200) reflections are amplified as an inset. It is seen that all the spectra fit the standard database for monoclinic lattice with the $P2/c$ group well, without an impurity phase detected in the apparatus resolution. The gradual lattice contraction accompanied with lattice distortion with increasing x is identified, as clearly seen in the inset. In Figs. 2(b) and 2(c) are shown the data for sample $x = 0.10$ as an example so that the main reflections are indexed for reference.

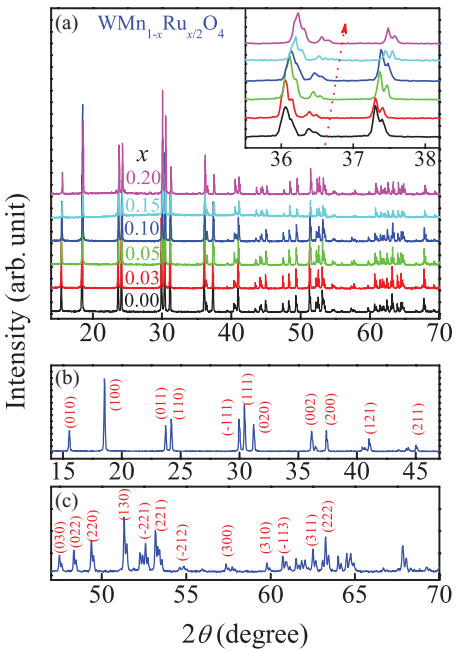

FIG. 2. (Color online) (a) Measured XRD spectra for a series of polycrystalline $Mn_{1-x}Ru_{x/2}WO_4$ samples with the numerical values for x. The inset shows the amplified local data with arrow indicating increasing x. The reflection indexing for sample $x = 0.10$ is given in (b) and (c).

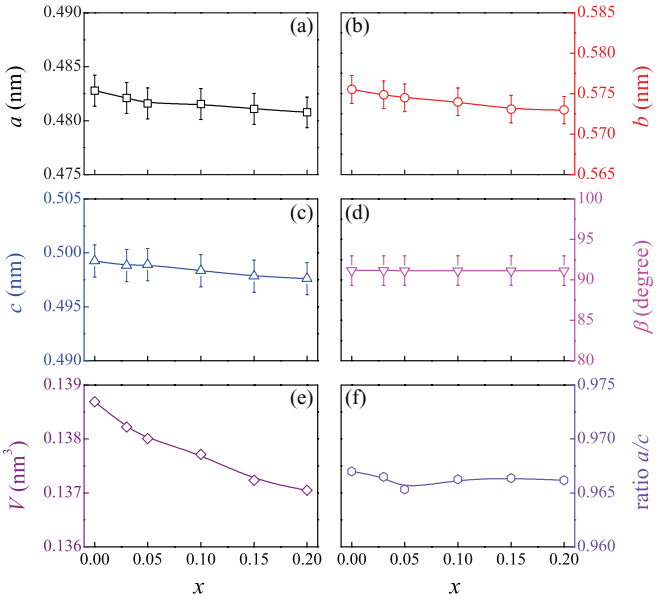

FIG. 3. (Color online) Evaluated lattice constants (a, b, c) and angle β between the a and c axes as a function of x, respectively, are shown in (a)–(d). The lattice unit volume V and ratio a/c are shown in (e) and (f).

For more clearly evaluating the lattice distortion upon the substitution, the three lattice constants and the angle β between the a and c axes as a function of x, respectively, are calculated from the refining process of the XRD data, and the results are presented in Figs. 3(a)–3(d). It is seen that lattice constants a, b, and c decrease gradually with increasing x, while angle β remains roughly unchanged. This indicates that the Ru^{4+} substitution does not seriously change the lattice symmetry although the atomic positions inside the unit cell cannot be precisely derived out from these changes. The present data do not allow an evaluation of either the length or the angle of the Mn(Ru)-O-Mn(Ru) bond, due to the limited apparatus resolution.

In Fig. 3(e) is plotted the lattice unit volume V as a function of x, evidencing its continuous decreasing. However, plotting ratio a/c as a function of x shows nearly no variation, consistent with the independence of angle β on x, as shown in Fig. 3(d). These results suggest that the lattice contraction upon the Ru^{4+} substitution is roughly isotropic, and one may argue that the helical spin rotation plane in the AF2 phase remains roughly unchanged in due course. Nevertheless, the lattice contraction should at least distort the zigzag Mn-Mn spin chain along the c axis with respect to that in $MnWO_4$, which can be a possible reason for the observed enhancement of polarization in the AF2 phase.

B. Specific heat and magnetic properties

We then investigate the variation of thermodynamic and magnetic properties of $Mn_{1-x}Ru_{x/2}WO_4$ with different values of x. The low-T data of specific heat $C_p(T)$ for several samples are plotted in Fig. 4(a). We have good reason to believe that the specific heat mainly comes from the contribution related to the excitation of spin structure. First, typical $C_p(T)$ curves with two λ-like magnetic phase transitions are shown for all

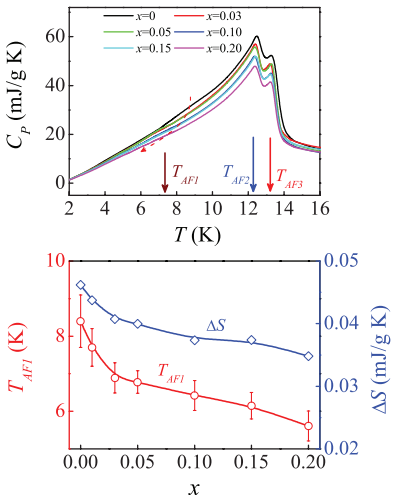

FIG. 4. (Color online) (a) Measured specific heat $C_p(T)$ in the low-T range for a series of samples, with T_{AF1}, T_{AF2}, and T_{AF3} labeled using arrows. (b) The evaluated TAF1 and entropy change ΔS over range (2 K, 16 K), as a function of x.

the samples. One transition occurs at $T = T_{AF3} \sim 13.3$ K, and the other at $T = T_{AF2} \sim 12.4$ K. The two transition points remain independent of the substitution level x. However, no peaklike anomaly as clear as that in single crystals at $T_{AF1} \sim 7$ K for sample $x = 0$ is observed. Instead, a weak and broad bumplike anomaly is identifiable there. This anomaly shifts remarkably downward the low-T side with increasing x, as indicated by the dashed arrow. It is suggested that the AF2 → AF1 transition is partially suppressed or delayed to the lower T side by the Ru^{4+} substitution. The estimated bump position designated as T_{AF1} in a function of x is plotted in Fig. 4(b) for reference, although the data show no good statistics.

Second, given the assumption that the specific heat mainly comes from the spin excitation, it is shown that the substitution downshifts the $C_P(T)$ curve, implying that the entropy associated with the spin structure is suppressed, i.e. the AF2 (AF3) phase is stabilized by the substitution. This tendency is very significant for the AF2 phase between T_{AF2} and T_{AF1}, as shown in Fig. 4(a). Taking the data for sample $x = 0$ as a reference, the entropy change ΔS over the T range (2 K, 16 K), evaluated from the $C_P(T)$ data, is presented in Fig. 4(b), too. It is clearly seen that $\Delta S(x)$ decreases gradually with increasing x, demonstrating the enhanced stability of the spin structure upon the Ru^{4+} substitution. In other words, the continuous decreasing of both $T_{AF1}(x)$ and $\Delta S(x)$ suggests that the spin frustration in $MnWO_4$ is reshuffled to some extent, or the AF2 phase becomes more stabilized, owing to the Ru^{4+} substitution, as argued earlier in Sec. I.

To further confirm the above effect, the magnetic behaviors of these $Mn_{1-x}Ru_{x/2}WO_4$ samples were investigated, and the data of magnetic susceptibility χ in both ZFC and FC modes for several samples are presented in Fig. 5. While not much quantitative information from the data can be evaluated, several interesting features are concerned. First, it is seen that the substitution remarkably suppresses the magnetic moment over the whole T range covered here. Although it is known that the Ru^{4+} ($\sim 2\ \mu_B$) has smaller moment than Mn^{2+} ($3.8 \sim 5.0\ \mu_B$),[24] the rapid fall of the moment at very low

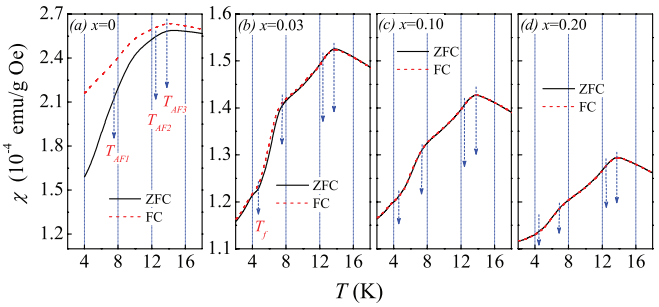

FIG. 5. (Color online) Measured magnetic susceptibility χ in both the ZFC and FC modes for (a) $x = 0$, (b) $x = 0.03$, (c) $x = 0.10$, and (d) $x = 0.20$. The arrows indicate the T_{AF1}, T_{AF2}, T_{AF3}, and a possible freezing point T_f. The measuring field is 1000 Oe.

x range ($x < 0.03$) implies an additional ingredient to the linear reduction of the moment in the high x range ($x > 0.05$). Second, it is noted that the moment separation between the ZFC and FC modes is very remarkable for sample $x = 0$ even above T_{AF3}; however, it nearly disappears at $x > 0.03$, and no more separation can be detected for $x > 0.05$. The overlapping of the ZFC and FC signals at least implies that the magnetic structure becomes more robust when the substitution is higher, noting that the measuring field is 1000 Oe and sufficient for reshuffling the spin configuration, if any, to some extent. Third, it is interesting to observe several anomalies in the χ-T curves of the substituted samples, corresponding to T_{AF3}, T_{AF2}, and even T_{AF1}, respectively. However, no such anomaly besides that at T_{AF3} for the pure $MnWO_4$ sample can be detected. This unusual feature reflects the fact that the magnetic structures in $MnWO_4$ are relatively soft, and the transitions between them can be diffusive. However, for the substituted samples, these transitions become sharp, and the magnetic structures, in particular the AF2 phase, are, respectively, favored highly.

It should be mentioned here that no detailed information on the spin structure evolution with decreasing T can be obtained only from the limited χ-T data. Nevertheless, based on these data, one may argue that the Ru^{4+} substitution does have an impact on the multifold interactions allowing the reshuffling of the spin configuration and thus enhances the robustness of at least one antiferromagnetic phase, respectively. In addition, the χ-T data show that T_{AF1} is downshifted with increasing x, coinciding with the behavior identified by the C_P-T data, i.e. the substitution prefers the AF2 phase rather than the AF1 phase, which is beneficial to ferroelectricity.

C. Dielectric and ferroelectric behaviors

Subsequently, we look at the dielectric and ferroelectric behaviors of the $Mn_{1-x}Ru_{x/2}WO_4$ samples. As examples, we first show the measured I-T curves for samples $x = 0.00$ and 0.20, as shown in Figs. 6(a) and 6(b), each for three different warming rates (1, 3, and 5 K/min), noting that the pyroelectric current is a quantity much more sensitive than polarization in response to variations of structure and spin order. For both cases, the measured current peaks and valleys/kinks at the three warming rates appear exactly at the same temperature without any shift, demonstrating that the measured signals do

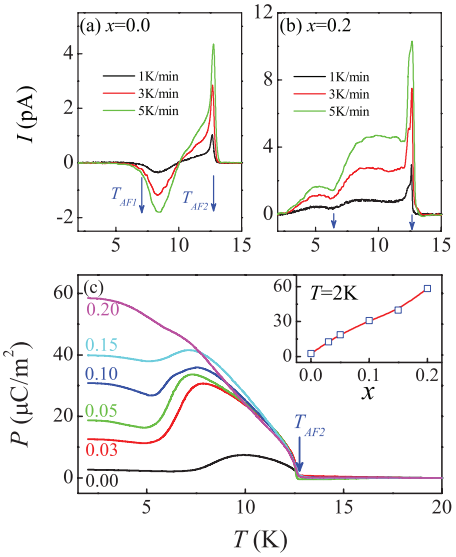

FIG. 6. (Color online) Measured pyroelectric current I as a function of T for (a) $x = 0.0$ and (b) $x = 0.2$ at three warming rates 1, 3, and 5 K/min, respectively. (c) The as-evaluated polarization P as a function of T for a series of samples with x labeled numerically. The P value at $T = 2$ K as a function of x is plotted in the inset.

come from the pyroelectricity. For sample $x = 0$, it is seen that the high-T peak is located exactly at T_{AF2}, marking the appearance of the AF2 phase, and the current disappearance occurs at T_{AF1}, indicating the replacement of the AF2 phase by the AF1 phase. For sample $x = 0.20$, the current initiates at T_{AF2}, and the kink is located at T_{AF1}.

The polarization, as evaluated by integrating the pyroelectric current as a function of T for all the samples, is then plotted in Fig. 6(c). The P-T data for sample $x = 0$ are quite similar to earlier results, and the polarization appears only within the AF2 phase between T_{AF2} and T_{AF1}.[27] The major consequence of the Ru substitution in terms of ferroelectricity is twofold. On one hand, similar to Co-substituted $MnWO_4$ and others,[31,37] polarization appears in the original AF1 phase regime (<7 K) because the AF1 phase is suppressed. On the other hand and more importantly, the polarization over the whole T range below T_{AF2} is remarkably enhanced, which has never been observed earlier. In earlier reports on the Co- or Zn-substituted $MnWO_4$, the measured P in the AF2 phase remains roughly unchanged,[31,37] although the AF2 phase regime extends into the AF1 phase of $MnWO_4$. In the present case, the peaked value of P in the AF2 phase is enhanced from ~7.0 $\mu C/m^2$ for sample $x = 0$ up to ~40 $\mu C/m^2$ for sample $x = 0.15$, noting that the samples are polycrystalline. At $x = 0.20$, it is seen that the whole T range below T_{AF2} is occupied with AF2 phase, and the maximal value of P reaches up to ~60 $\mu C/m^2$, almost one order of magnitude larger than pure $MnWO_4$. In the inset of Fig. 6(c), the measured P at $T = 2$ K as a function of x is plotted.

A significant difference of the Ru substitution from earlier reported Co or Zn substitution in $MnWO_4$ is that a tiny Co or Zn substitution (<2%) is sufficient to completely suppress the AF1 phase, allowing the AF2 phase to occupy the whole T range below T_{AF2}.[31,37] For the Ru substitution, it is seen that the AF1 phase is gradually suppressed, but a substitution

up to $x = 0.15$ is not yet enough to remove the AF1 phase, although the induced polarization is already much larger than the Co- or Zn-substituted systems. The kink feature of the P-T data at $T \sim 6$ K for all substituted samples allow us to infer the coexistence of the AF1 and AF2 phases below $T \sim 6$ K, which is not observable in Co- or Zn-substituted systems. These results suggest that the Ru substitution may bring an additional ingredient into the mechanism for multiferroicity in $MnWO_4$, which is quite different from the $3d$ substitution.

Furthermore, both the specific heat and magnetic data obtained under zero or nonzero magnetic field do not show any feature other than those from the AF1, AF2, and AF3 phases, which implies that the Ru^{4+} substitution does not bring an additional magnetic phase.[37]

D. Magnetoelectric coupling

The argument of phase coexistence in $Mn_{1-x}Ru_{x/2}WO_4$ can be further checked by the magnetoelectric (ME) coupling effect. While the response of P of $MnWO_4$ itself to H was investigated, we present here the data for two samples $x = 0.05$ and 0.15 in Fig. 7. As reported in Ref. 27, for pure $MnWO_4$,

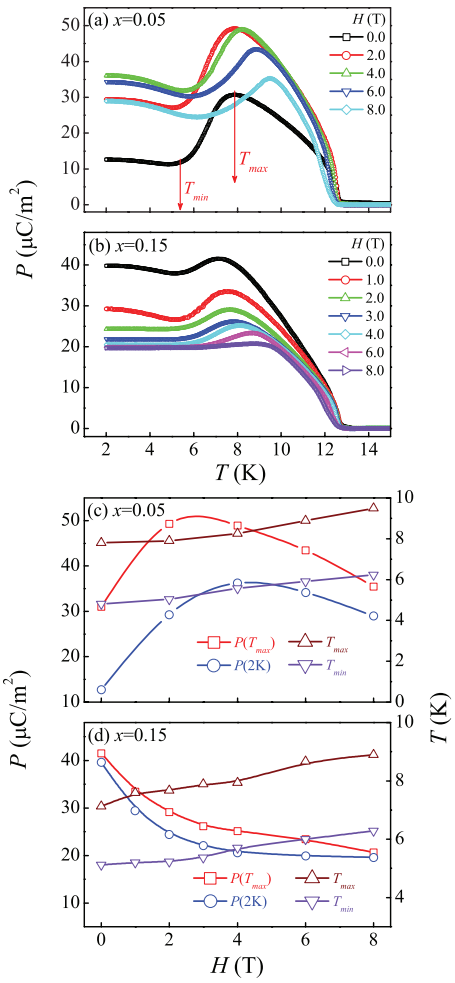

FIG. 7. (Color online) Measured polarization P in response to H for two samples (a) $x = 0.05$ and (b) 0.15. The evaluated $P(T_{max})$, $P(T = 2\,K)$, T_{max}, and T_{min} are plotted in (c) for sample $x = 0.05$ and (d) for $x = 0.15$.

a field applied along the b axis suppresses remarkably the AF2 phase and thus the polarization along the b axis, but a polarization flip leads to the appearance of polarization along the a axis, although the a-axis polarization is much smaller than that along the b axis.

For this paper, we deal with the polycrystalline samples. Quite different ME response is seen. For sample $x = 0.05$, the magnetic field first raises the polarization over the whole T range below T_{AF2} until $H = 4.0$ T, beyond which a gradual suppression of the polarization is observed. We plot the maximal polarization in the AF2 phase at T_{max} and that at $T = 2$ K as a function of H, respectively, in Fig. 7(c), where the two temperature points T_{max} and T_{min} (corresponding to the minimal polarization) are plotted, too. Indeed, both $P(T_{max})$ and $P(2\,K)$ as a function of H show a maximal at $H = 3$ and 4 T, respectively, while T_{max} and T_{min} shift slightly towards the high-T side.

The situation for sample $x = 0.15$ becomes different again, as shown in Figs. 7(b) and 7(d). The measured P over the whole T range below T_{AF2} is gradually suppressed with increasing H. Similar to sample $x = 0.05$, T_{max} and T_{min} shift slightly towards the high-T side. However, it is interesting to note that the polarization is suppressed down to a plateau at $H = 8$ T. Considering the fact that the AF1 phase is fragile to H,[26,27] one may argue that this polarization plateau comes purely from the AF2 phase over the whole T range below T_{AF2}, while the AF2 phase can survive under a field as high as $H = 11$ T.[38]

The above results allow us to argue again that the $Mn_{1-x}Ru_{x/2}WO_4$ samples do accommodate the coexisting AF1 and AF2 phases below T_{AF2}, although additional and more direct imaging evidence is needed to conclude this argument. In addition, due to the polycrystalline nature of the samples, we cannot obtain sufficient knowledge on the polarization flip from the b axis to the a axis under magnetic field. However, such a flip does not contribute additional polarization larger than that along the b axis. Therefore, the polarization enhancement under low H for sample $x = 0.05$ should not come from this flip sequence. Details of the mechanisms for the ME effect will be discussed preliminarily, but more investigation is needed.

E. Phase diagram

To this stage, we can evaluate the magnetic phase diagrams for the $Mn_{1-x}Ru_{x/2}WO_4$ series on the (x,T) and (H,T) planes, respectively. Based on all of the measured data, the proposed phase diagrams are still more or less semiquantitative, and quantitatively reliable phase diagrams require more data on the spin structure and phase coexistence.

Figure 8(a) shows the x-T phase diagram at $H = 0$, where the AF1 phase disappears and the AF1 + AF2 mixed regime appears immediately upon the substitution. From our data, no change of the boundary between the AF2 phase and AF3 phase is identified, and the AF1 + AF2 mixed regime is suppressed as x is up to 0.20, as shown in Fig. 6. The H-T phase diagrams for samples $x = 0.05$ and 0.15 as two examples are presented in Figs. 8(b) and 8(c), respectively. It is seen that the two samples have slightly different phase diagrams. Clearly, the lower x sample has more extensive AF1 + AF2 coexisting regime, and in particular the AF1 phase can survive at low H, which cannot, however, be possible in the higher x sample.

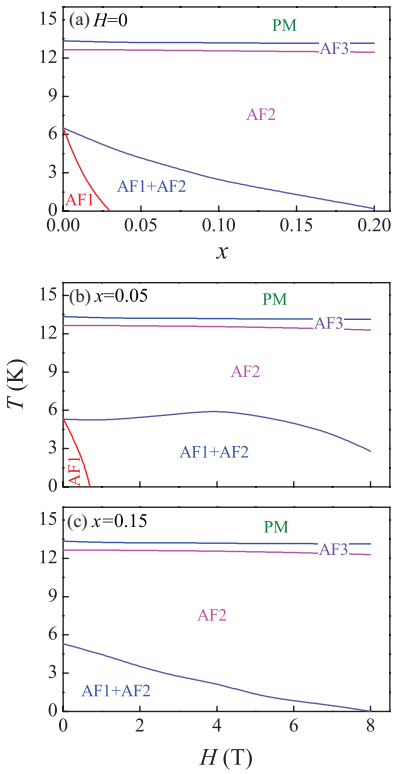

FIG. 8. (Color online) Proposed phase diagrams on (a) the T-x plane at $H = 0$, (b) the T-H plane for $x = 0.05$, and (c) the T-H plane for $x = 0.15$, respectively. PM denotes the paramagnetic state.

It is also suggested that the AF2 phase occupies a broader regime in the higher-x sample, reflecting the fact that the AF1 phase is destabilized by the Ru^{4+} substitution accompanied by the remarkably enhanced stability of the AF2 phase.

As discussed above, as a 4d transition metal species, Ru^{4+} has more extensive electron density distribution and contributes stronger SOC effect than the 3d ions.[33] These effects together with the induced lattice contraction are responsible for the observed phenomena. Since no details on the Ru substitution relevant spin structure are available, here we may only be able to provide a qualitative discussion on the polarization enhancement in the AF2 phase upon the substitution. Consulting the Mn-Mn spin chain as revealed by neutron scattering and shown in Fig. 1,[37] one sees the possible reasons for the polarization enhancement. First, the SOC constant A can become bigger upon the Ru^{4+} substitution. This is an important ingredient for enhancing the polarization. Second, the enhanced p-d hybridization between the Mn(Ru) and O species may also contribute to the polarization enhancement.[34]

Needless to mention, an oversubstitution of Mn by Ru would eventually break all the Mn spin-related phases, and instead the Ru spin-dominated magnetic phase ensues. Regarding the magnetic field response of the polarization, one argues that a similar mechanism to $MnWO_4$ applies here. The magnetic field first destabilizes the AF1 phase, allowing the partial occupation of the AF1 phase regime by the AF2 phase. The pure AF1 phase regime is also completely removed in the high-x samples, as illustrated by the phase diagrams in Fig. 8(c). Nevertheless, the microscopic reason for the AF1 destabilization and AF2 stabilization in $Mn_{1-x}Ru_{x/2}WO_4$ is still open.

IV. CONCLUSION

In conclusion, we have performed detailed measurements of the multiferroic behaviors of 4d Ru^{4+}-substituted $Mn_{1-x}Ru_{x/2}WO_4$ in polycrystalline form. Our focus was the ferroelectricity enhancement and spin-order modulation as a consequence of the Ru substitution. Our experiments have revealed that the Ru^{4+} substitution leads to the lattice contraction and suppresses the magnetization. The nonferroelectric AF1 phase is destabilized and partially replaced with the ferroelectric AF2 phase, resulting in the coexisting AF1 + AF2 regime. Different from the 3d species-substituted $MnWO_4$,[28–31] the Ru substitution enhances remarkably the polarization by almost one order of magnitude, and the magnetoelectric response behavior depends on the substitution level. This paper discusses multiferroic phenomena other than the $MnWO_4$ doped by the 3d transition metal ions such as Co, Zn, and Fe, etc.

ACKNOWLEDGMENTS

This work was supported by the National 973 Projects of China (Grants No. 2011CB922101 and No. 2009CB623303), the Natural Science Foundation of China (Grants No. 11234005 and No. 11074113), and the Priority Academic Program Development of Jiangsu Higher Education Institutions, China.

*Corresponding author: liujm@nju.edu.cn

[1] Y. Tokura, Science **312**, 1481 (2006).
[2] S. W. Cheong and M. Mostovoy, Nat. Mater. **6**, 13 (2007).
[3] K. F. Wang, J. M. Liu, and Z. F. Ren, Adv. Phys. **58**, 321 (2009); S. Dong and J. M. Liu, Mod. Phys. Lett. **26**, 1230004 (2012).
[4] T. Kimura, T. Goto, H. Shintani, T. Arima, and Y. Tolura, Nature (London) **426**, 55 (2003).
[5] T. Goto, T. Kimura, G. Lawes, A. P. Ramirez, and Y. Tokura, Phys. Rev. Lett. **92**, 257201 (2004).
[6] N. Hur, S. Park, P. A. Shama, J. S. Ahn, S. Guha, and S. W. Cheong, Nature (London) **429**, 392 (2004).
[7] S. Park, Y. J. Choi, C. L. Zhang, and S. W. Cheong, Phys. Rev. Lett. **98**, 057601 (2007).
[8] T. Kimura, J. C. Lashley, and A. P. Ramirez, Phys. Rev. B **73**, 220401(R) (2006).
[9] K. Kimura, H. Nakamura, S. Kimura, M. Hagiwara, and T. Kimura, Phys. Rev. Lett. **103**, 107201 (2009).
[10] G. Lawes, A. B. Harris, T. Kimura, N. Rogado, R. J. Cava, A. Aharony, O. Entin-Wohlman, T. Yildrim, M. Kenzelmann, C. Broholm, and A. P. Ramirez, Phys. Rev. Lett. **95**, 087205 (2005).
[11] L. Lin, Y. J. Guo, Y. L. Xie, S. Dong, Z. B. Yan, and J. M. Liu, J. Appl. Phys. **111**, 07D901 (2012).

[12]I. A. Sergienko and E. Dagotto, Phys. Rev. B **73**, 094434 (2006).
[13]H. Katsura, N. Nagaosa, and A. V. Balatsky, Phys. Rev. Lett. **95**, 057205 (2005).
[14]M. Kenzelmann, A. B. Harris, S. Jonas, C. Broholm, J. Schefer, S. B. Kim, C. L. Zhang, S. W. Cheong, O. P. Vajk, and J. W. Lynn, Phys. Rev. Lett. **95**, 087206 (2005).
[15]S. G. Condran and M. L. Plumer, J. Phys.: Condens. Matter **22**, 162201 (2005).
[16]S. Ishiwata, Y. Kaneko, Y. Tokunaga, Y. Taguchi, T. H. Arima, and Y. Tokura, Phys. Rev. B **81**, 100411(R) (2010).
[17]V. Y. Pomjakushin, M. Kenzelmann, A. Dönni, A. B. Harris, T. Nakajima, S. Mitsuda, M. Tachibana, L. Keller, J. Mesot, H. Kitazawa, and E. Takayama-Muromachi, New J. Phys. **11**, 043019 (2009).
[18]T. C. Han and H. H. Chao, Appl. Phys. Lett. **97**, 232902 (2010).
[19]S. Dong, R. Yu, S. Yunoki, J. M. Liu, and E. Dagotto, Phys. Rev. B **78**, 155121 (2008).
[20]M. Mochizuki and N. Furukawa, Phys. Rev. B **80**, 134416 (2009).
[21]C. R. dela Cruz, B. Lorenz, Y. Y. Sun, Y. Wang, S. Park, S. W. Cheong, M. M. Gospodinov, and C. W. Chu, Phys. Rev. B **76**, 174106 (2007).
[22]R. P. Chaudhury, B. Lorenz, Y. Q. Wang, Y. Y. Sun, and C. W. Chu, New J. Phys. **11**, 033036 (2009).
[23]N. Zhang, Y. Y. Guo, L. Lin, S. Dong, Z. B. Yan, X. G. Li, and J. M. Liu, Appl. Phys. Lett. **99**, 102509 (2011).
[24]G. Lautenschläger, H. Weitzel, T. Vogt, R. Hock, A. Böhm, M. Bonnet, and H. Fuess, Phys. Rev. B **48**, 6087 (1993); A. H. Arkenbout, T. T. M. Palstra, T. Siegrist, and T. Kimura, *ibid.* **74**, 184431 (2006).
[25]H. Ehrenberg, H. Weitzel, H. Fuess, and B. Hennion, J. Phys.: Condens. Matter **11**, 2649 (1999).
[26]K. Taniguchi, N. Abe, H. Sagayama, S. Otani, T. Takenobu, Y. Iwasa, and T. Arima, Phys. Rev. B **77**, 064408 (2008).
[27]K. Taniguchi, N. Abe, T. Takenobu, Y. Iwasa, and T. Arima, Phys. Rev. Lett. **97**, 097203 (2006).
[28]R. P. Chaudhury, B. Lorenz, Y. Q. Wang, Y. Y. Sun, and C. W. Chu, Phys. Rev. B **77**, 104406 (2008).
[29]Y. S. Song, J. H. Chung, J. M. S. Park, and Y. N. Choi, Phys. Rev. B **79**, 224415 (2009).
[30]H. Weitzel, Solid State Commun. **8**, 2071 (1970).
[31]R. P. Chaudhury, F. Ye, J. A. Fernandez-Baca, B. Lorenz, Y. Q. Wang, Y. Y. Sun, H. A. Mook, and C. W. Chu, Phys. Rev. B **83**, 014401 (2011).
[32]F. Ye, Y. Ren, J. A. Fernandez-Baca, H. A. Mook, J. W. Lynn, R. P. Chaudhury, Y. Q. Wang, B. Lorenz, and C. W. Chu, Phys. Rev. B **78**, 193101 (2008); K. C. Liang, Y. Q. Wang, Y. Y. Sun, B. Lorenz, F. Ye, J. A. Fernandez-Baca, H. A. Mook, and C. W. Chu, New J. Phys. **14**, 073028 (2012).
[33]V. Durairaj, S. Chikara, X. N. Lin, A. Douglass, G. Cao, P. Schlottmann, E. S. Choi, and R. P. Guertin, Phys. Rev. B **73**, 214414 (2006).
[34]S. Seki, N. Kida, S. Kumakura, R. Shimano, and Y. Tokura, Phys. Rev. Lett. **105**, 097207 (2010).
[35]C. Y. Ren, Phys. Rev. B **79**, 125113 (2009).
[36]G. Zhang, S. Dong, Z. Yan, Y. Guo, Q. Zhang, S. Yunoki, E. Dagotto, and J. M. Liu, Phys. Rev. B **84**, 174413 (2011).
[37]F. Ye, S. X. Chi, J. A. Fernandez-Baca, H. B. Cao, K. C. Liang, Y. Q. Wang, B. Lorenz, and C. W. Chu, Phys. Rev. B **86**, 094429 (2012).
[38]B. Kundys, C. Simon, and C. Martin, Phys. Rev. B **77**, 172402 (2008).